Surface imaging by carbon monoxide field desorption

J. A. Panitz[a)]
University of New Mexico School of Medicine, Department of Cell Biology, Albuquerque, New Mexico 87131

J. J. Hren
North Carolina State University, Department of Material Science and Engineering, Raleigh, North Carolina 27615-7907

(Received 30 September 1986; accepted 8 December 1986)

The morphology of a field-emitter tip has been visualized in atomic resolution for the first time at a field strength below 15 V/nm. Images are generated by continuous field desorption of a physisorbed carbon monoxide monolayer. The monolayer is replenished at 25 K by CO adsorption from the gas phase. High-contrast images are obtained by time gating for CO^+ (the dominant field-desorbing species) in the imaging atom probe. Images integrated over several hundred field-desorption events show morphology at the center of large (thermally annealed) flat, crystal planes, and document the decrease in spatial resolution that accompanies pulsed-laser imaging of surface adsorbates. CO desorption images demonstrate that high-field imaging is no longer restricted to edge, kink site, and protruding atoms on the surface of a field-emitter tip.

I. INTRODUCTION

The field-ion microscope is a powerful tool for examining the surface of a solid in atomic resolution.[1] With the introduction of the atom probe,[2] and the imaging atom probe,[3] element identification and its mapping on a subnanometer scale became possible. Although these techniques can visualize the surface of a field-emitter tip in exquisite detail, most observations are complicated by the high electric field that is required for analysis. At a typical imaging field ($F > 22$ V/nm), a very large electrostatic field stress $F^2/8\pi > 10^{10}$ dyn/cm^2) exists at the tip apex, distorting the substrate lattice and displacing surface atoms from their equilibrium positions. Although most gas phase species are ionized in space without reaching the tip surface, polarizable species (such as hydrogen and helium) will accelerate to the tip apex, and may bind to high-field regions of the surface by a field-induced dipole–dipole bond.[4] An unstressed, clean, adsorbate-free surface does not exist in the field-ion microscope under best imaging conditions.

This paper explores the use of physisorbed carbon monoxide to image the surface of a field-emitter tip. During imaging, the electrostatic field stress at the tip surface is greatly reduced, and field adsorption is a negligible phenomenon. Imaging is not restricted to high-field regions of the surface. As a result, surprisingly detailed images are obtained at the center of large, flat, crystal planes where the local field strength is too low for field-ion imaging to be effective.

II. SURFACE IMAGING WITH FIELD-ADSORBED HELIUM

Field-adsorbed helium will preferentially bind to the same surface atoms that are imaged in the field-ion microscope (i.e., at edge, kink site, and protruding atoms) where the highest local field strengths are generated.[5] Below 80 K, field adsorption always occurs under field-ion imaging conditions.[6] The strength of a field-adsorption bond depends on the temperature of the tip apex and the strength of the electric field at its surface. For example, at 20 K field adsorption will always occur at surface sites where the local electric field strength is greater than ~ 17 V/nm.[7] If the local electric field strength at the tip surface is increased (at a fixed temperature), or if the temperature of the tip is increased (at a constant field strength), the field-adsorption bond can be broken, and field-adsorbed helium will desorb from the tip surface as a positive ion. An image that reflects the location of field-adsorbed helium on the tip surface prior to desorption can be obtained in the field-ion microscope if the microscope is equipped with a detector that can image individual ions.[8]

Since the strength of a field-adsorption bond will increase with increasing field strength, field-adsorbed helium can only be removed from the tip apex (below ~ 80 K) if the lattice is dissolved by a process known as *field evaporation*.[9] Since field evaporation will change the surface with each desorption event, this type of image (integrated over many desorption events to minimize random noise) cannot be used to visualize the position of surface atoms. To visualize surface atoms, field-adsorbed helium must be removed from a tip without changing the underlying substrate. This can be accomplished by using a short-duration laser pulse to heat the surface and initiate a desorption event at a constant field strength that is below the evaporation field of the substrate.

A pulsed-laser desorption image using field-adsorbed helium to visualize the surface looks remarkably similar to a field-ion image of the surface taken with helium as the imaging gas.[10] The images look similar because helium field adsorbs at the same high-field positions on the surface that are imaged in the field-ion microscope. The resolution of a pulsed-laser desorption image is inferior to its field-ion counterpart because the temperature of the tip apex is raised by the laser pulse to initiate the desorption event. The higher surface temperature increases the tangential velocity component of the desorbing ions which reduces the spacial resolution of the desorption image.[11]

 0734-2101/87/041032-04$01.00 © 1987 American Vacuum Society

III. SURFACE IMAGING WITH PHYSISORBED CO

A desorption image that uses field-adsorbed helium to visualize the surface of a field-emitter tip is not more informative than a field-ion image of the surface because the desorption image visualizes the same protruding surface atoms that are seen in the field-ion image, but at lower resolution. The imaging procedure described in this paper is unusual in that it produces an image of the tip surface in which surface atoms that cannot be seen in a field-ion image are visualized with a comparable resolution. To accomplish this, a monolayer of CO is *physisorbed* on the tip surface at 20 K from the gas phase and then field desorbed without increasing the temperature of the tip or changing its surface morphology. The resulting image, immune from field-adsorption phenomena, maps the desorption probability of CO within the physisorbed layer. Surprisingly, the image also reflects the structure of the underlying surface in atomic resolution.

Under our experimental conditions, CO can chemisorb (and will physisorb) on the tip apex from the gas phase, but will not field adsorb or condense to form a thick layer of frozen CO ice. Field adsorption of gas phase CO does not occur during the imaging process because a relatively low-field strength is required to remove CO from the surface, and the field is usually present only during the duration of the desorption pulse. Since the pulse lasts for ~ 50 ns, there is not enough time (at a typical CO partial pressure of 1×10^{-7} Torr) to field adsorb a monolayer of CO on the tip surface. Since field adsorption does not dominate the imaging process, CO desorption images reflect subtle features of surface morphology. It is interesting to note that Müller anticipated this type of desorption imaging when he introduced the field-ion microscope in 1951.[12]

IV. EXPERIMENTAL CONSIDERATIONS

The imaging atom probe (shown schematically in Fig. 1) was used for this investigation.[13] Field desorption was initiated by applying a high-voltage pulse of positive polarity to the tip. The pulse amplitude could be varied between 0.5 and 2.0 kV. For some tips (of large radius) the required desorption field was established by supplementing the maximum pulse amplitude with a dc bias added directly to the tip. The dc bias, when present, was not large enough to cause CO to field adsorb on the tip surface. Although the width of the desorption pulse was ~ 50 ns, the actual duration of a desorption event has been shown to be ~ 4 ns.[14]

Mass spectra were obtained by recording the travel time of field-desorbed species on a transient waveform oscilloscope. The start of a desorption pulse triggered the oscilloscope sweep and provided a fiducial mark that indicated the instant of desorption (within 5 ns). The mass-to-charge ratio m/z of each field-desorbed species was calculated from the equation[15]:

$$m/z = 0.193(V_{dc} + V_{pulse})(T/d)^2,$$

where $(V_{dc} + V_{pulse})$ is measured in kilovolts; d the distance between the tip and the detector (that records their arrival) in meters, and T the travel time of the ion in microseconds. An accuracy of 0.5 amu and a mass resolution of 1 amu (for $m/z < 30$ amu) were obtained in these experiments.

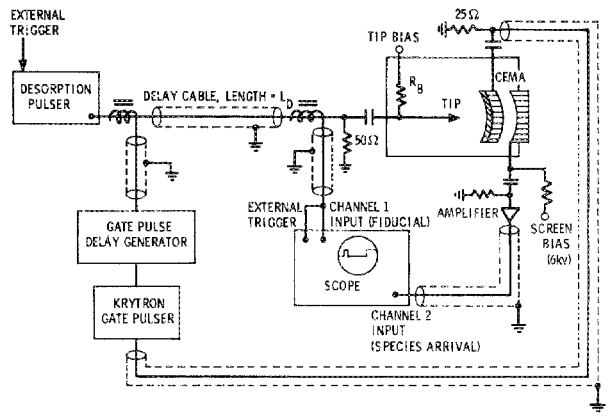

FIG. 1. A schematic drawing of the imaging atom probe. Mass spectra are obtained by recording the travel time of field-desorbed species between the tip and a spherically curved (chevron) microchannel plate detector having single-ion detection sensitivity. A preselected species on the surface of the tip apex can be imaged in atomic resolution by time gating the detector coincidently with its arrival. (See Ref. 15.)

Desorption images were obtained by placing a photographic emulsion (Polaroid type 57 film) in direct contact with the fiberoptic faceplate of the chevron, microchannel plate detector. The detector was time gated for $m/z = 28$ to eliminate random noise from the image (CO^+ was the dominant species desorbing from the surface). Several hundred desorption images were photographically integrated at the detector by applying a number of desorption pulses ($= N_p$) to the tip, equally spaced in time. The pulse interval ($= T_p$) was adjusted to maximize the number of CO^+ ions in each desorption image. The number of CO^+ ions was a function of the partial pressure of CO in the gas phase, the pulse interval, and the total surface area from which ions were collected. As the pulse interval was increased, the number of CO^+ ions increased and then remained constant (within 1%–2%) indicating that a saturation coverage of CO on the surface was being maintained. The tip temperature (T_{tip}) could be adjusted from 15–80 K (and maintained within 5 K) by a closed-cycle, liquid-helium refrigerator and in-vacuum specimen heater.[16]

V. RESULTS AND DISCUSSION

In order to estimate the CO^+ desorption field, mass spectra were taken of the species desorbed from the tip surface as a function of tip bias. At a low tip bias (V_1), only CO^+ was seen in the mass spectra of the desorbing physisorbed layer. At a significantly higher tip bias (V_2), H^{2+} was detected. If the H^{2+} desorption field F_H is assumed to be ~ 20 V/nm,[17] then the CO^+ desorption field F_{CO} can be estimated from the ratio of the tip bias at which the two species were desorbed. From a typical experiment:

$$F_{CO} \sim F_H (V_1/V_2) = 20(3000/5200) = 11 \text{ V/nm}. \quad (1)$$

Equation (1) indicates that a CO^+ desorption image will occur at almost one-half of the field strength required for field-ion imaging in hydrogen, and less than one-quarter of the vacuum evaporation field of tungsten.[18] At this field

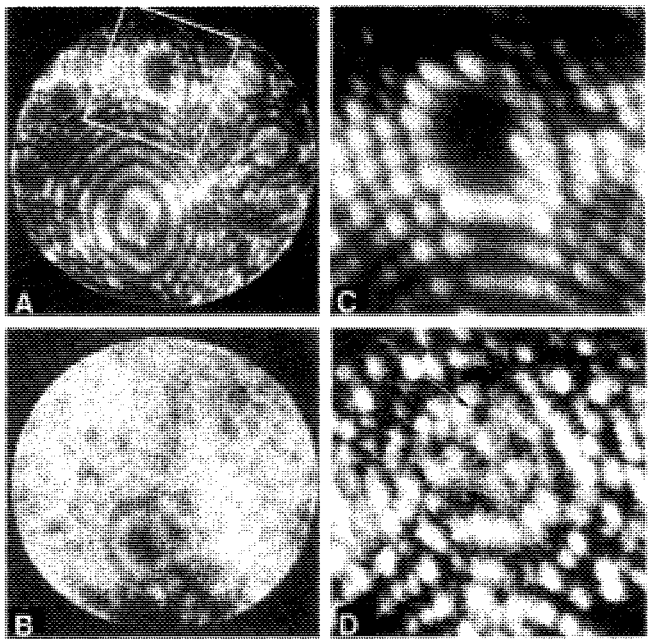

FIG. 2. A comparison of field-ion imaging, field desorption imaging with field-adsorbed hydrogen, and field-desorption imaging with physisorbed CO. (a) A field-ion image of a (110)-oriented tungsten tip taken in helium at 5.5 kV. $P_{\text{helium}} = 1\times10^{-6}$ Torr, $T_{\text{tip}} = 20$ K. (b) A field-desorption image of the same tip, time gated for H_2^+. $P_{\text{hydrogen}} = 1\times10^{-7}$ Torr, $N_p = 250$, $T_p = 2$ s, $T_{\text{tip}} = 20$ K. (c) An enlargement of the surface area outlined in the helium field-ion image. (d) A field-desorption image of the same surface area, time gated for CO^+. $P_{CO} = 1\times10^{-7}$ Torr, $N_p = 2500$, $T_p = 0.1$ s, $T_{\text{tip}} = 20$ K.

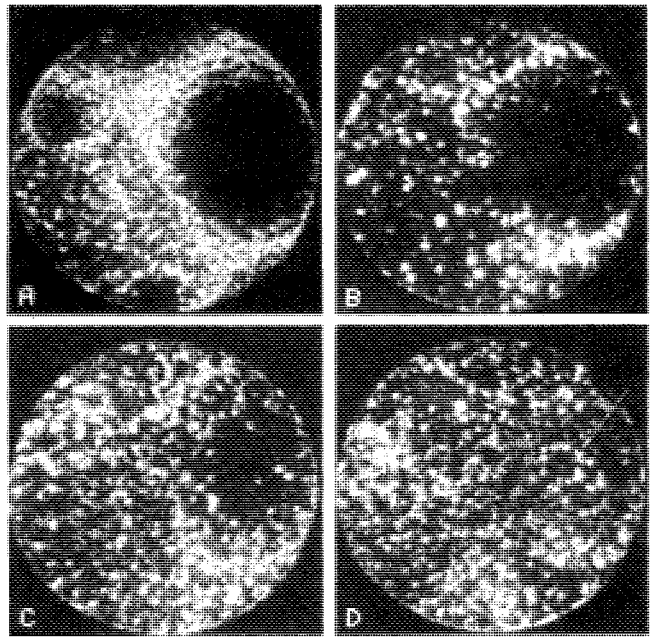

FIG. 3. A comparison of field-ion image of a large radius tungsten tip with field-desorption images of the same tip at increasing desorption field strengths. (a) A field-ion image of the tip taken in helium at 20 kV. $P_{\text{helium}} = 3\times10^{-6}$ Torr, $T_{\text{tip}} = 20$ K. (b) A field-desorption image of the same tip, time gated for CO^+. $P_{\text{tip}} = 7.3$ kV, $P_{CO} = 1.4\times10^{-7}$ Torr, $N_p = 999$, $T_p = 0.1$ s, $T_{\text{tip}} = 20$ K. (c) A field-desorption image of the same tip, time gated for CO^+. $V_{\text{tip}} = 8.3$ kV, $P_{CO} = 1.4\times10^{-7}$ Torr, $N_p = 999$, $T_p = 0.1$ s, $T_{\text{tip}} = 20$ K. (d) A field-desorption image of the same tip, time gated for CO^+. $V_{\text{tip}} = 9.3$ kV, $P_{CO} = 1.4\times10^{-7}$ Torr, $N_p = 999$, $T_p = 0.1$ s, $T_{\text{tip}} = 20$ K. The arrow points toward a feature that appears to be a small crystal plane. Only the edge atoms of the plane are visible.

strength, field adsorption of gas phase CO is improbable, even at 20 K.[19]

Figure 2 compares field-ion imaging of a tungsten tip with field-desorption imaging of the same tip using both field-adsorbed hydrogen, and carbon monoxide as imaging species. Figure 2(a) is a field-ion micrograph of a tungsten tip taken at 5.5 kV. Figure 2(b) is a desorption micrograph time gated for H_2^+. An H^{2+} image does not show the prominent kink-site atoms that are visualized in a field-ion image, probably because a large fraction of field-adsorbed hydrogen originates at nonapex sites on the surface.[20] Figure 2(c) is an enlargement of the region outlined in Fig. 2(a). Figure 2(d) is a CO^+ desorption micrograph taken within the outlined region of the surface. Morphology within the plane is clearly visualized in this image, but is not seen in the field-ion micrograph. It is tempting to associate the dark regions at the center of the plane with vacancies or interstitials at the surface. One possible vacancy is indicated with an arrow in Fig. 2(d).

Since a desorption image time gated for CO^+ reflects structure on relatively smooth regions of the tip apex, we decided to use the same method to look at the center of very large, flat crystal planes on thermally annealed tungsten tips. The center of large, flat crystal planes cannot be imaged by field-ion microscopy. Tips were prepared by thermally annealing a small radius tungsten tip, in vacuum, at ~2800 K for ~60 s. Figure 3(a) is a field-ion micrograph of such a tip taken at 20 kV. Figures 3(b)–3(d) are desorption micrographs of the same tip, time gated for CO^+, and taken as a function of increasing tip bias. Figure 3(b) was taken at 7.3 kV. Figure 3(c) was taken at 8.3 kV. Figure 3(d) was taken at 8.3 kV. The arrow in Fig. 3(d) points to a feature that resembles a field-ion image of a small, circular crystal plane where only the edge atoms are imaged.

At a low tip bias, a CO^+ desorption image of a large radius tip looks like a field-ion image of the surface. The dark regions in both images [e.g., Figs. 3(a) and 3(b)] are the large, flat crystal planes produced by the annealing process. The bright regions are the regions of high curvature on the surface that bound the crystal planes and join them together to form the overall shape of the tip apex. As the tip bias is increased, a CO^+ desorption image visualizes more detail in the smoother regions of the tip apex. This behavior can be qualitatively understood as follows: At low tip potentials, the desorption field for CO is established first at high-field regions of the surface (i.e., regions where the local radius of curvature is large). These are the same regions that are imaged in the field-ion microscope, so both images look similar. As the tip bias is increased, the field required for CO desorption is established in the flat, smooth regions of the surface (i.e., progressively closer to the center of the large,

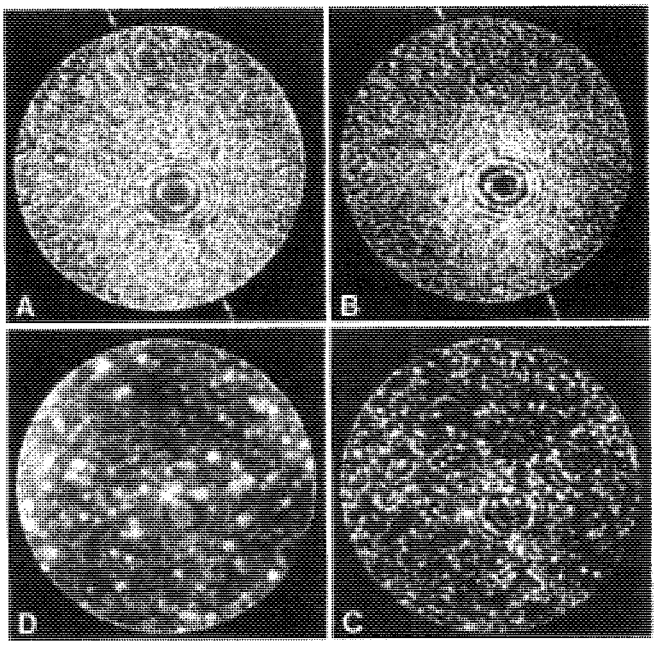

FIG. 4. A comparison of a field-ion image of a tungsten tip, with field-desorption images of the tip (and a pulsed-laser desorption image of the tip) taken at elevated temperatures. (a) A field-ion image of the tip taken in helium at 14 kV. $P_{\text{helium}} = 1\times10^{-6}$ Torr, $T_{\text{tip}} = 20$ K. (b) A field-desorption image of the same tip, time gated for CO^+, taken at 20 K. $P_{CO} = 1\times10^{-7}$ Torr, $N_p = 999$, $T_p = 0.1$ s. A grain boundary (indicated by the arrows) is visible in both images. (c) A field-desorption image of the same tip, time gated for CO^+, taken at 47 K. $P_{CO} = 1\times10^{-7}$ Torr, $N_p = 999$, $T_p = 0.1$ s. (d) A 4-μJ, pulsed-laser desorption image of the same tip, taken at 20 K. $P_{CO} = 1\times10^{-7}$ Torr, $N_p = 100$, $T_p = 0.1$ s. The loss in image resolution in the latter two images is associated with an increased surface temperature during the desorption event.

flat crystal planes), and more detail in these regions is observed. Eventually, a tip potential is established that corresponds to the minimum field strength required for CO desorption over the entire imaged area of the tip. At this field strength the entire surface of the tip apex is imaged.

Field-ion imaging in helium cannot be used to image the entire surface of a thermally faceted tip because the regions of high curvature will field evaporate before field-ion imaging conditions are established at the center of the large crystal planes (the best imaging field for tungsten in helium is 70% of its evaporation field). If field-ion imaging in hydrogen is attempted, the field at the surface can be substantially increased before the tungsten surface field evaporates, but the entire surface will not be resolved because optimal imaging conditions occur only over a very narrow field range (corresponding to a very narrow range of surface topography).

The temperature dependence of a CO^+ desorption image was also investigated. Figure 4(a) is a field-ion micrograph of an (011) tungsten tip taken at 20 K. Figure 4(b) is a CO^+ desorption micrograph of the same tip taken $\sim$1 h later at the same temperature. Note the grain boundary (indicated by an arrow) in both images. The ability to resolve a grain boundary (that crosses different surface morphologies) in both images indicates that the physisorbed layer in the CO^+ image is not thick enough to obscure subtle details of surface topography, and suggests that the surface is not changed by the presence of CO on the surface during the imaging process.

The resolution of a CO^+ desorption image is comparable to the resolution of a field-ion image at 20 K. At 30 K the loss in resolution of the desorption image begins to be noticed; above 40 K most surface detail in the desorption image is lost. This is seen in Fig. 4(c) which is a CO^+ desorption micrograph taken at 47 K. Figure 4(d) shows the effect of heating the tip surface with a 4-μJ laser pulse to initiate desorption. The image, time gated for CO^+, was taken at 20 K but looks like the CO^+ image taken at 47 K. The desorption rate of CO from the surface was about the same under both imaging conditions, suggesting that the laser pulse increased the surface temperature by $\sim$27 K.[21] This observation may have important consequences for surface imaging in the pulsed-laser atom probe.[22]

The resolution of a pulsed-laser desorption image is always worse than a voltage-pulsed image because the laser increases the surface temperature during the desorption event. A comparison of Figs. 4(b) and 4(d) emphasizes this point and highlights the need to minimize the amplitude of the laser pulse when the distribution of a species on the apex of a field-emitter tip is being imaged in the pulsed-laser atom probe. If the pulse amplitude is arbitrarily large, the surface temperature during the desorption event will be large, and the resolution of the desorption image will suffer. A large temperature excursion could also induce thermal migration of surface species during the desorption event, causing a preselected species to be incorrectly visualized in a desorption image of the surface.

[a] Visiting Research Professor; on sabbatical leave of absence from Sandia National Laboraties, Albuquerque, NM 87185.

[1] T. T. Tsong, J. Electron. Microsc.Technol. **2**, 229 (1985).
[2] E. W. Müller, J. A. Panitz, and S. B. McLane, Rev. Sci. Instrum. **39**, 83 (1968).
[3] J. A. Panitz, J. Vac. Sci. Technol. **11**, 206 (1974).
[4] E. W. Müller, J. A. Panitz, and S. B. McLane, Surf. Sci. **17**, 430 (1970).
[5] E. W. Müller and T. T. Tsong, in *Progress in Surface Science*, edited by S. Davison (Pergamon, New York, 1973), Vol. 4, p. 40.
[6] T. T. Tsong and E. W. Müller, J. Chem. Phys. **55**, 2889 (1971).
[7] T. T. Tsong and E. W. Müller, Phys. Rev. Lett. **25**, 911 (1970).
[8] J. A. Panitz, J. Vac. Sci. Technol. **12**, 210 (1975).
[9] E. W. Müller and T. T. Tsong, *Field-Ion Microscopy: Principles and Applications* (Elsevier, New York, 1969), p. 56.
[10] G. L. Kellogg and T. T. Tsong, Surf. Sci. Lett. **110**, L599 (1981).
[11] See Ref. 9, p. 35.
[12] E. W. Müller, Z. Phys. **131**, 136 (1951).
[13] J. A. Panitz, in *Progress in Surface Science*, edited by S. Davidson (Pergamon, New York, 1978), Vol. 3, p. 219.
[14] J. A. Panitz and R. J. Walko, Rev. Sci. Instrum. **47**, 1251 (1976).
[15] J. A. Panitz, in *Methods of Experimental Physics*, edited by R. L. Park and M. Lagally (Academic, New York, 1985), Vol. 22, p. 349.
[16] G. L. Fowler and J. A. Panitz, Rev. Sci. Instrum. **51**, 1730 (1980).
[17] T. T. Tsong, T. J. Kinkus, and C. F. Ai, J. Chem. Phys. **78**, 4768 (1983).
[18] See Ref. 9, p. 72.
[19] T. T. Tsong and E. W. Müller, Phys. Rev. Lett. **25**, 910 (1970).
[20] G. L. Kellogg and T. T. Tsong, Surf. Sci. Lett. **110**, L604 (1981).
[21] G. L. Kellogg, J. Appl. Phys. **52**, 5320 (1981).
[22] G. L. Kellogg, J. Phys. E **20**, 125 (1987).